

Organic light-emitting materials and devices for optical communication technology

Hiroyuki Suzuki*

NTT Photonics Laboratories, NTT Corporation, 3-1 Morinosato Wakamiya, Atsugi, Kanagawa, 243-0198, Japan

Received 29 October 2003; received in revised form 14 January 2004; accepted 5 April 2004

Abstract

This paper outlines our recent efforts to develop organic infrared (IR) and near-infrared (NIR) light-emitting materials and devices for use in optical communication technology. The IR and NIR light-emitting materials investigated are two organic ionic dyes, (2-[6-(4-dimethylaminophenyl)-2,4-neopentylene-1,3,5-hexatrienyl]-3-methyl-benzothiazonium perchlorate) (LDS821) and $[C_{41}H_{33}Cl_2N_2]^+ \cdot BF_4^-$ (IR1051), and an organic rare-earth complex, erbium (III) tris(8-hydroxyquinoline) (ErQ). These materials exhibit photo- and electro-luminescence in the 0.8-, 1.1- and 1.5- μm wavelength regions, respectively. They were used as optically active species in the following three device forms; vacuum-deposited or doped spin-coated polymer thin-films, doped monodispersed polymer microparticles, and embedded polymeric optical waveguides with a doped core. I propose possible optical communication applications based on their optical properties and luminescent processes.

© 2004 Elsevier B.V. All rights reserved.

Keywords: Organic IR light-emitting materials; Organic rare-earth complex; Organic ionic dyes; Polymer optical waveguides; Polymer microparticles; Optical communication

1. Introduction

Optical technology has brought about a remarkable improvement in the transmission capacity of backbone networks using the wavelength-division multiplexing (WDM) scheme, which is unattainable with electrical technology. Worldwide competition is underway to develop various optical devices with a view to achieving similar innovations in node systems for ultrafast and large-capacity information processing. There is also an ongoing challenge to realize organic light-emitting materials and devices for use in optical communication technology. However, only a limited role can be expected for organic materials as regards applications to backbone networks. This is mainly because, backbone networks achieve long-distance transmission through silica optical fibers using their minimal transmission loss in the 1.5- μm wavelength region. Recent demands for optical technology to be introduced into access and home networks have increased the relative importance of organic materials and devices with respect to their alternatives since these networks require low-cost devices and transmit optical signals only over short distances using the NIR

or even visible regions. Although, organic light-emitting materials in the visible region have already established their solid position owing to their successful use in organic electro-luminescence (EL) devices, scientists are now being drawn towards those in the NIR and IR regions as a result of technological movements in optical communication [1,2].

The organic IR and NIR light-emitting materials that have been reported so far, are organic ionic dyes [3–5], organic rare-earth complexes comprising a central trivalent rare-earth ion, such as Er^{3+} [6,7], Nd^{3+} [8,9], or Pr^{3+} [10] and organic ligands, and semiconductor nanoparticles with organic substituents [11–13]. Organic rare-earth complexes exhibit photo-luminescence (PL) and EL in the 1.0–1.6- μm region originating from the radiative 4f–4f transitions of the rare-earth ions that they contain [14]. Ionic dyes are the only examples, where the IR and NIR luminescence originate from organic components. However, there are few ionic dyes that show luminescence longer than 1.2 μm in solid films. Semiconductor nanoparticles exhibit emission in the 1.3- μm region from core semiconductor nanocrystals. Thus, the luminescence of organic rare-earth complexes can meet the required wavelength for long distance transmission applications whereas the others are suitable solely for transmission over limited distances. Materials exhibiting luminescence longer than 1 μm can also be used with

* Tel.: +81 46 240 3533; fax: +81 46 240 4300.
E-mail address: hiroyuki@aecl.ntt.co.jp (H. Suzuki).

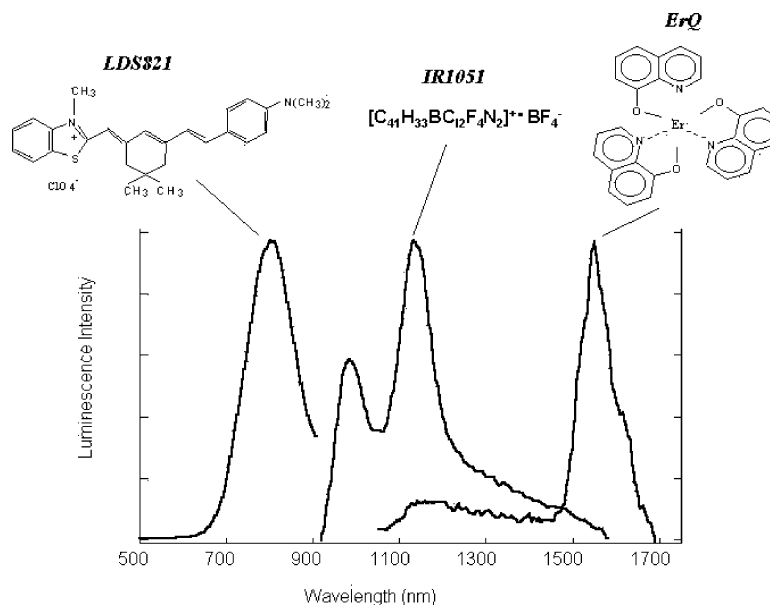


Fig. 1. Molecular structures and luminescence spectra of the IR and NIR light-emitting materials used in this study. Only the structural formula of $[C_{41}H_{33}Cl_2N_2]^+ \cdot BF_4^-$ is provided for IR1051. The spectra shown are EL for LDS821 and IR1051, and PL for ErQ.

silicon-based photonic crystal circuits where μm -range propagation is expected.

This paper examines the PL and EL characteristics of organic IR and NIR light-emitting materials in various device forms. These materials include two organic ionic dyes, 2-[6-(4-dimethylaminophenyl)-2,4-neopentylene-1,3,5-hexatrienyl]-3-methyl-benzothiazonium perchlorate (LDS821) and $[C_{41}H_{33}Cl_2N_2]^+ \cdot BF_4^-$ (IR1051), and an organic rare-earth complex, erbium (III) tris(8-hydroxyquinoline) (ErQ). I prepared polymer films, monodispersed polymer microparticles, and polymer embedded optical waveguides, all of which were doped with these materials. I also made vacuum-deposited films of ErQ. These dye-doped polymer microparticles and optical waveguides are examples of cavities combined with organic optically active materials, and are promising in terms of realizing various types of novel organic optical devices capable of operating in the IR and NIR regions. I propose possible device applications for use in optical communication networks by considering the device structure (thin-film or waveguide device) and the excitation mode (current and optical excitation) with reference to their optical properties and luminescent processes.

2. Experiments

The molecular structures of LDS821, IR1051, and ErQ are shown in Fig. 1. LDS821 (Exciton Laser Dyes,) and IR1051 (Aldrich) were obtained commercially and used without further purification. ErQ was synthesized by mixing erbium (III) chloride in aqueous solution with 8-hydroxyquinoline (8-Q) in methanol. PBD (Dojindo Laboratories, scintillator grade) and PVK (Aldrich, secondary standard) were

also used as an electron transporting material and a hole transporting host polymer for EL measurements. These IR and NIR light-emitting materials were used in various device forms, namely, in vacuum-deposited films (only for ErQ), doped spin-coated polymer films (for LDS821 and IR1051), doped monodispersed polymer microparticles, and polymer embedded optical waveguides with doped cores. The doped dye concentration was 1 wt.% for all the samples used in the present work. I used conventional photolithography and O_2 reactive ion etching (RIE) to fabricate polymer optical waveguides using UV-curable acrylate and epoxy polymers as IR and NIR transparent matrices [15]. Dye-doped monodispersed microparticles with diameters of 0.4–19.2 μm , were prepared by seeded polymerization. I examined the luminescence properties of these samples at room temperature using previously reported apparatuses [5,16].

3. Results

3.1. Luminescence properties of organic ionic dye-doped samples

The luminescence process in two organic dyes is described within the framework of that in conventional organic light-emitting materials in other wavelength regions. Photoexcited states deactivate either radiatively or nonradiatively to the ground state, and the luminescence spectra are mirror images of the absorption spectra.

3.1.1. Luminescence properties of LDS821-doped samples

I first describe the EL characteristic of LDS821 [3]. The EL spectrum of LDS821, which coincides well with its

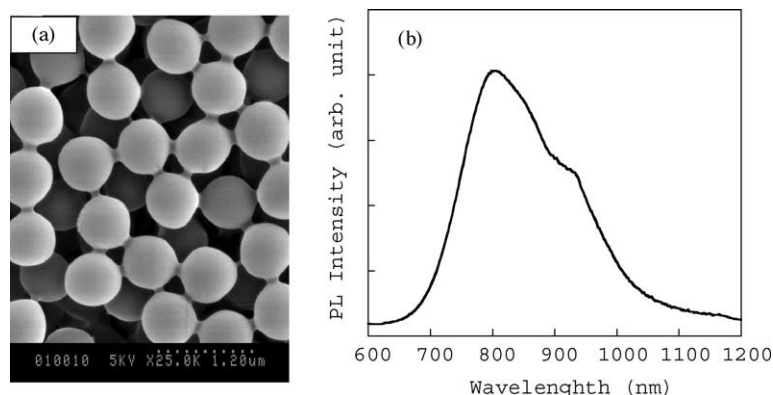


Fig. 2. SEM photograph of LDS821-doped microparticles (diameter: $0.4\ \mu\text{m}$) (a) and their PL spectrum (b).

PL spectrum, is shown in Fig. 1. Spectroscopic and ionization potential measurements revealed that the ionization potential and the bandgap energy were 5.2 and 2.1 eV for LDS 821, 5.8 and 3.6 eV for PVK, respectively, and so the LDS821 doped in PVK acted as an effective carrier trapping and radiative recombination center for the EL. With Al and ITO electrodes, the EL quantum efficiency of LDS821 is 0.015% photons/electron with a PBD concentration of 30 wt.%. When measured under a constant current, the EL intensity (and therefore the EL quantum efficiency) changed markedly with time and reverse bias voltage. The EL intensity became up to 80 times larger than its initial value and the EL quantum efficiency reached the 1% photons/electron level. This behavior has been ascribed to enhanced electron and hole injection caused by strong internal fields effective at the interfaces between PVK and two injecting electrodes induced by the doped ionic dye alignment along the bias field [3,17]. The same type of EL enhancement has also been observed for several other ionic emissive dyes [18,19].

Fig. 2a is a photograph of LDS821-doped monodispersed PMMA microparticles (diameter: $0.4\ \mu\text{m}$) taken with a scanning electron microscope (SEM). I was able to detect $0.8\ \mu\text{m}$ PL from polymer microparticles doped with LDS821 (see Fig. 2b). This indicates that the polymer microparticles were successfully doped with the dye molecules. LDS821-doped embedded optical waveguides made of UV-curable epoxy resin possess a low propagation loss region around $0.8\ \mu\text{m}$ (see Fig. 3a), which corresponds with the emission wavelength of LDS821. The optical propagation loss of an LDS821-doped waveguide (core size: $8.5\ \mu\text{m} \times 8.5\ \mu\text{m}$) was measured, and found to be 0.15 dB/cm at $0.83\ \mu\text{m}$. This indicates that it can be used as a light-emitting device in the NIR region.

3.1.2. Luminescence properties of IR1051-doped samples

The EL spectrum of PVK doped with IR1051 is shown in Fig. 1. This spectrum contains two distinct emission bands peaking at around 1.0 and $1.5\ \mu\text{m}$ [5]. Spectroscopic and ionization potential measurements revealed that the ioniza-

tion potential and bandgap energy were, 4.5 and 1.1 eV for the monomer IR1051, 6.0 and 4.1 eV for PBD, and 5.8 and 3.6 eV for PVK, respectively, as shown in Fig. 4. The doped IR1051, thus acted as an effective carrier trapping and radiative recombination center for the EL. The EL band at around $1.0\ \mu\text{m}$ is ascribable to the dimer IR1051 [4,5].

IR1051-doped monodispersed PMMA microparticles (diameter: $0.6\ \mu\text{m}$) exhibit a distinct $1.1\text{-}\mu\text{m}$ PL, indicating again that the polymer microparticles were successfully doped with the dye. Fig. 5 is a cross-sectional SEM

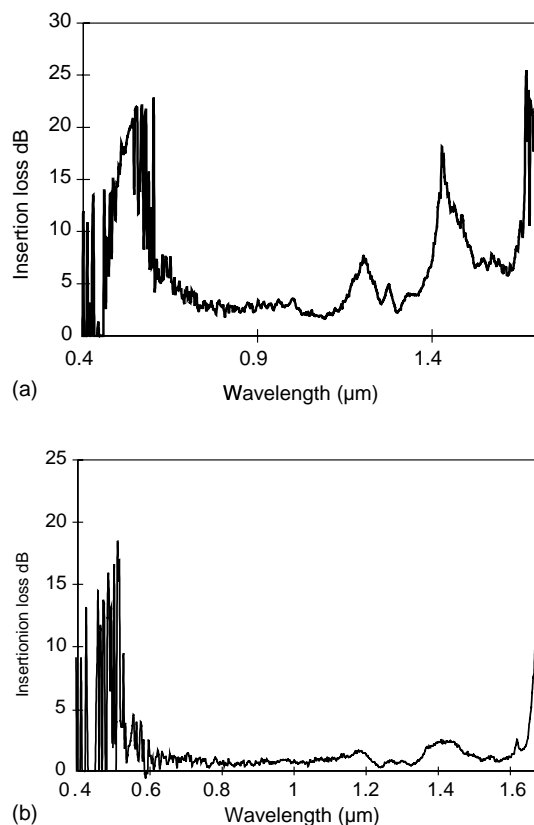


Fig. 3. Insertion loss spectrum of the 10 mm long (a) LDS821-doped and (b) ErQ-doped waveguide.

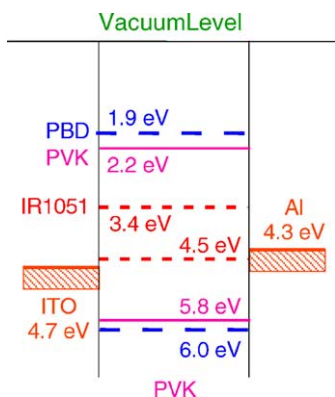


Fig. 4. Band diagram of ITO/IR1051(1 wt.%), PBD (30 wt.%):PVK/Al.

photograph of an embedded UV-curable epoxy resin optical waveguide with an IR1051-doped core (core size: $7.5 \mu\text{m} \times 7.5 \mu\text{m}$). The waveguide has a low propagation loss region around $1.1 \mu\text{m}$ that corresponds to the emission wavelength of IR1051. The optical propagation loss of an IR1051-doped waveguide (core size: $7.2 \mu\text{m} \times 7.5 \mu\text{m}$) was measured and found to be 0.06 dB/cm at $0.83 \mu\text{m}$. This again indicates that it can be used as a light-emitting device in the NIR region.

3.2. Luminescence properties of ErQ-doped samples

Fig. 1 shows the PL spectrum of a vacuum-deposited ErQ film in the IR region. I detected two PL bands at around 1.2 and $1.55 \mu\text{m}$ [16,20], which are assigned to the $^4\text{S}_{3/2} \rightarrow ^4\text{I}_{11/2}$ and $^4\text{I}_{13/2} \rightarrow ^4\text{I}_{15/2}$ transitions, respectively [14]. I also detected many emission bands between the visible and NIR regions in vacuum-deposited ErQ films [20]. In contrast to the organic ionic dyes discussed above, the PL process in ErQ is dominated by a ligand-sensitization mechanism (see Fig. 6) where the $1.54 \mu\text{m}$ emission originates from the $^4\text{I}_{13/2}$ state of Er^{3+} populated by the efficient excited energy transfer from the triplet excited states of the organic ligands [21,22]. This was confirmed by a marked intensity enhancement for the $1.54 \mu\text{m}$ PL that resulted from shifting

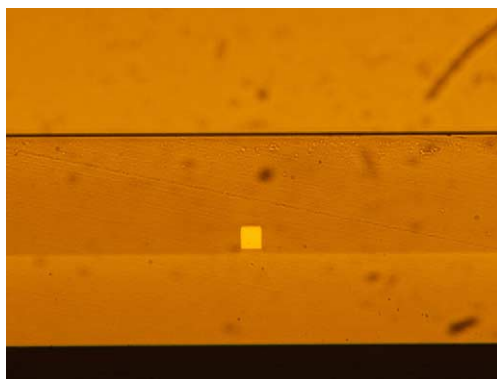


Fig. 5. Cross-sectional SEM photograph of the IR1051-doped embedded waveguide with a $7.5 \mu\text{m} \times 7.5 \mu\text{m}$ core.

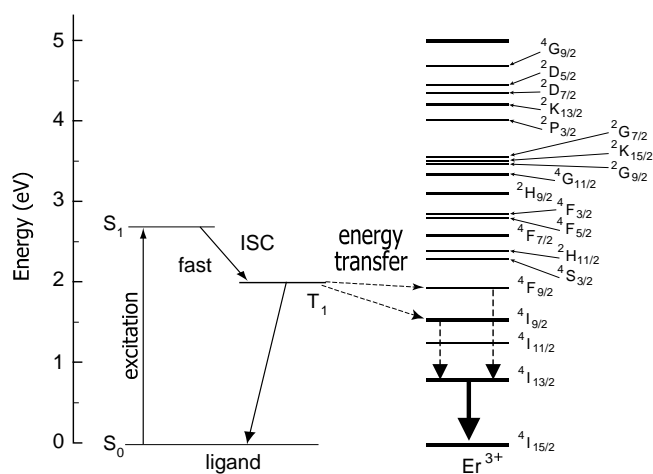


Fig. 6. Schematic drawing of the ligand-sensitized photoluminescence process in ErQ.

the excitation wavelength from 514.5 to 405 nm , as shown in Fig. 7a. The absorption spectrum of ErQ reveals that the dominant photoexcited species change from Er^{3+} to organic ligands (8-Q) in accordance with the excitation wavelength shift from 514.5 to 405 nm . The concentration of photoexcited species is therefore greatly increased by the shorter wavelength excitation, since the transition of the organic ligand is allowed while the Er^{3+} transitions are forbidden.

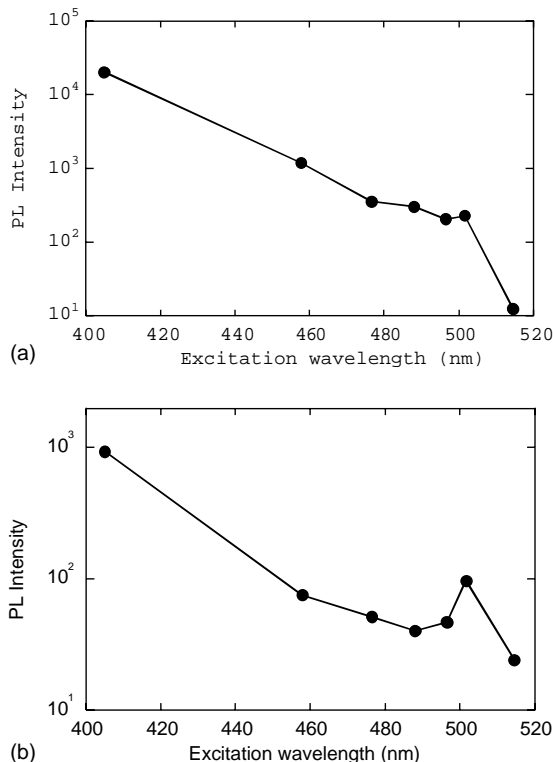


Fig. 7. The excitation wavelength dependence of the $1.55 \mu\text{m}$ PL intensity for (a) a vacuum-deposited ErQ thin-film and (b) 1 wt.% ErQ-doped PMMA microparticles with a diameter of $0.8 \mu\text{m}$.

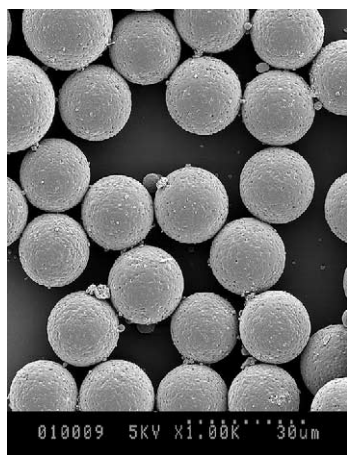


Fig. 8. SEM photograph of ErQ-doped microparticles (diameter: 19.2 μm).

This ligand-sensitized PL mechanism is unique to organic rare-earth complexes and can be utilized to enhance the PL intensity originating from the 4f–4f forbidden transitions of the rare-earth ions that they contain.

Fig. 8 is a SEM photograph of ErQ-doped monodispersed PMMA microparticles (diameter: 19.2 μm). I was

able to detect 1.54 μm PL for ErQ-doped polymer microparticles with diameters of 0.8 and 19.2 μm [16]. As with the vacuum-deposited ErQ film described above, a PL enhancement was observed for the 1.54 μm PL with both sizes of polymer microparticles. Fig. 7b is the result for ErQ-doped polymer microparticles with a diameter of 0.8 μm . Once more these observations show that the polymer microparticles were successfully doped with ErQ and that the ligand-sensitization scheme can also operate in these material systems. ErQ-doped embedded optical waveguides made of UV-curable acrylate possess a low propagation loss region around 1.5 μm that corresponds to the emission wavelength of ErQ, as shown in Fig. 3b. The optical propagation loss of an ErQ-doped waveguide (core size: 7.2 $\mu\text{m} \times 6.9 \mu\text{m}$) was measured and found to be 0.7 dB/cm at 1.55 μm for both the TE and TM modes. Fig. 9 shows near-field mode pattern (NFP) of the waveguide (core size: 7.2 \times 8.1 μm) together with the intensity distribution of the NFP along the x and y axes. The intensity distribution can be well-fitted with a Gaussian curve for the two axes: (FWHM: $x = 5.2 \mu\text{m}$, $y = 6.0 \mu\text{m}$; $1/e^2$: $x = 9.4$, 10.5 μm), indicating that it is a single-mode waveguide at 1.55 μm [15].

4. Discussion

The dye-doped thin-films (either vacuum-deposited or spin-coated) discussed above, can be used for thin-film devices, such as EL devices since all the materials have been confirmed to be IR or NIR electro-luminescent. The EL quantum efficiency is currently less than 1% for LDS821, and orders of magnitude smaller for the two IR materials. Device structure optimization can improve the EL efficiency, but there is still the challenge of developing IR and NIR light-emitting materials with an improved EL quantum efficiency. For instance, the EL of LDS821 and IR1051 contains a visible component together with the NIR or IR component [3,5]. For instance, the visible EL intensity shares 60% of the total EL intensity for IR1051. The visible EL reduces the IR or NIR EL intensity, because these two EL processes compete with each other as the radiative excited states of the ionic dyes generated by the electron-hole recombination. This is also true for ErQ, since its EL contains a visible component in addition to the 1.54 μm EL [7]. Moreover, this material system poses a substantial problem in that the EL originates from the parity-forbidden 4f–4f transitions of Er^{3+} . This is even more problematic for thin-film devices, such as EL devices where only a limited number of rare-earth ions can be utilized for the emission. The ligand-sensitization scheme observed for the optical excitation of the organic ligands is a way to solve the problem, but has not been confirmed to occur in current excitation. To realize the ligand-sensitization scheme in the current excitation, carriers must be injected into the conduction and valence bands of organic ligands. Since,

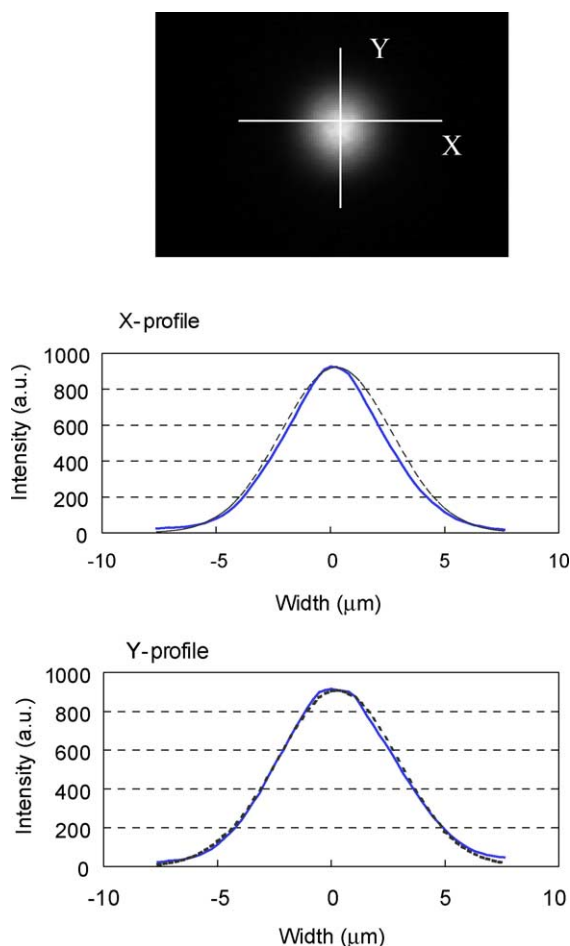


Fig. 9. Near field mode pattern of the ErQ-doped waveguide with a 7.2 $\mu\text{m} \times 8.1 \mu\text{m}$ core.

the bandgap of organic ligands is normally large, the effective injection of carriers into organic ligands is difficult to achieve and so the EL efficiency thus generated, is low. The roadmap for optical communication technology anticipates the use of 0.8 μm light for home network applications in the form of light-emitting diodes (LED) or laser diodes (LD) with a direct modulation speed of 0.5–1.6 Gbit/s together with polymer optical fibers (POFs) [23]. 1.1 μm light can also be used for home networks as well as local area networks because both silica and POFs have a reasonably low transmission loss for short-distance transmission. However, organic light-emitting materials in these wavelength regions have to compete with their semiconductor counterparts already in practical use. Therefore, we must develop device forms unique to organic materials, such as planar LEDs or LDs. These device forms must be suitable for organic materials in terms of processability, and be able to increase the transmission bandwidth by space division multiplexing.

The waveguide structure is another major device structure that has been practically utilized in a wide variety of optically active devices. Waveguide devices rely on the enhanced interaction between light and optically active species through effective light confinement. The magnitude of the interaction is increased with increases in the concentration of the optically active species and the waveguide length. This type of structure is particularly important for optical devices based on organic rare-earth complexes as regards improving the device characteristics since they exhibit PL principally as a result of forbidden transitions. A typical example is a rare-earth doped optical fiber amplifier where inorganic glass fibers are doped with a comparatively low concentration of rare-earth ions to obtain a high optical gain [14].

The application of ErQ to optically active waveguide devices operated by optical excitation has several advantages in that the number of rare-earth ions available for optically active functions can be increased, and the ligand-sensitization scheme can be directly used to enhance the PL efficiency by choosing the pumping wavelength. The wavelength of pumping lasers can be tuned by changing the structure of organic ligands attached to the central Er^{3+} through material engineering. In addition, high-power compact pumping light sources are easily available from the IR to UV regions. I suggest a compact optical waveguide amplifier as a possible application target suitable for ErQ operated by optical excitation. Recently, there has been an increasing demand for compact and low-cost optical amplifiers with a comparatively small gain of about 10 dB to compensate for the loss caused by the use of an optical device (insertion loss) and/or to introduce the WDM scheme into broadband optical access networks utilizing optical fibers. IR polymers can be doped with ErQ at a concentration of a few wt.%, and the device length can be reduced. The uniqueness of organic materials makes it possible for ErQ-doped polymers to have a two-dimensional (2D) structure thus enabling us to realize planar optical waveguide amplifiers. Another advantage of ErQ as regards optical amplifier use is its PL bandwidth,

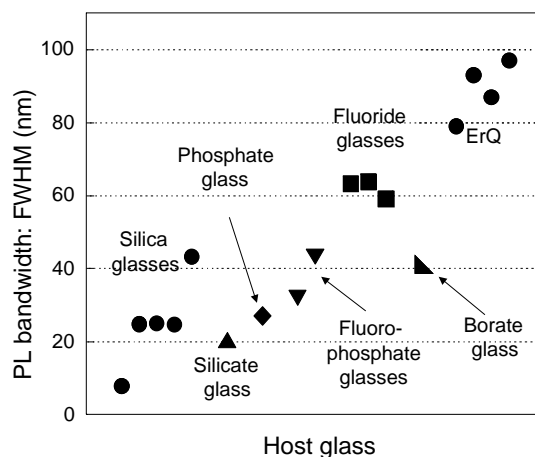


Fig. 10. PL bandwidth of Er^{3+} in various host matrices.

which is an approximate measure of the optical amplification bandwidth. The PL bandwidths of all the ErQ samples (80–100 nm) are larger than those (8–64 nm) of Er^{3+} in various inorganic glass matrices exhibiting optical amplification [14,16], as shown in Fig. 10. The larger PL bandwidths in these ErQ samples originate from the more inhomogeneous nature of ErQ and/or the polymer matrices.

Another attractive target for future research, is to combine a cavity structure with these IR and NIR light-emitting materials in order to control their emission characteristics and thus realize novel optically active devices. The cavity structures that I adopted are the polymer microparticles and optical waveguides discussed above. Dye-doped polymer waveguides provide the potential to realize optically excited lasing with a simple Fabry-Perot or distributed feedback (DFB) structure. Polymer microparticles doped with optically active molecules were recently used as optically pumped lasing media [24]. Photonic crystal-like characteristics were also reported in highly ordered self-assembled arrays of polymer microparticles [25]. Another example of a cavity is a photonic crystal. In previous studies, we adopted a photonic crystal (PhC) structure as a cavity and introduced three types of PhC structure into organic emissive materials in the visible region, either by hybridization [26,27] or nano-imprinting [28]. We realized an organic 2D PhC laser [26] and a nano-imprinting organic PhC laser whose lasing threshold can be controlled by the magnitude of the imprinting pressure [28]. We also observed a sharp emission (FWHM: 3 nm) from the defect levels in a 2D PhC [27]. All three PhC structures can be combined with at least the IR1051 and ErQ examined in this work, and research in this direction is planned for the future.

5. Conclusion

The luminescence properties of three IR and NIR light-emitting materials, LDS821, IR1051, and ErQ were examined in three device forms; vacuum-deposited thin-films,

doped spin-coated polymer films, and doped polymer microparticles. I observed the same luminescence characteristics for all these forms, including ligand sensitized PL in ErQ. I also fabricated polymer embedded optical waveguides with doped cores and confirmed that there were good propagation properties in the luminescence wavelength regions. I discussed the advantages and limits of these materials for use in optically active devices for photonic communications. I also suggested that the unique properties of organic Er complexes can be best utilized by optical excitation in waveguide structures, such as low-cost and compact optical waveguide amplifiers, rather than in applications operated by current excitation. Another application target for these light-emitting materials could be a novel light-emitting device realized by combining them with a cavity structure, such as polymer microparticles and PhCs. Research on the development of organic light-emitting materials in the IR and NIR regions is still in its preliminary stage, and further efforts to optimize materials and device structures will lead to success in developing optically active devices for use in optical communication technology.

Acknowledgements

I thank Soken Chemical & Engineering Co. Ltd., and NTT Advanced Technology Corporation for their help in fabricating the dye-doped microparticles and waveguides, respectively.

References

- [1] H. Suzuki, Res. Adv. Appl. Phys. 3 (2003) 11–25.
- [2] H. Suzuki, M. Notomi, A. Yokoo, Polym. Adv. Technol. 15 (2004) 75–80.
- [3] H. Suzuki, Appl. Phys. Lett. 76 (2000) 1543–1545.
- [4] M. Casalbani, F. De Matteis, P. Proposito, R. Pizzoferrato, Appl. Phys. Lett. 75 (1999) 2172–2174.
- [5] H. Suzuki, Appl. Phys. Lett. 80 (2002) 3256–3258.
- [6] W.P. Gillin, R.J. Curry, Appl. Phys. Lett. 74 (1999) 798–799.
- [7] R.J. Curry, W.P. Gillin, Appl. Phys. Lett. 75 (1999) 1380–1382.
- [8] O.M. Khreis, R.J. Curry, M. Somerton, W.P. Gillin, J. Appl. Phys. 88 (2000) 777.
- [9] Z. Hong, C. Liang, R. Li, F. Zang, D. Fan, W. Li, L.S. Hung, S.T. Lee, Appl. Phys. Lett. 79 (2001) 1942–1944.
- [10] Y. Kawamura, Y. Wada, Y. Hasegawa, M. Iwamuro, T. Kitamura, S. Yanagida, Appl. Phys. Lett. 74 (1999) 3245–3247.
- [11] N. Tessler, V. Medvedev, M. Kazes, S. Kan, U. Banin, Science 295 (2002) 1506–1508.
- [12] Y.-W. Cao, U. Banin, Angew. Chem. Int. Ed. 38 (1999) 3692–3694.
- [13] Y.-W. Cao, U. Banin, J. Am. Chem. Soc. 122 (2000) 9692–9702.
- [14] M.J.F. Digonnet (Ed.), Rare-Earth Doped Fiber Lasers and Amplifiers, Marcel Dekker, New York, 1993.
- [15] M. Hikita, H. Suzuki, Jpn. J. Polym. Sci. Tech. 61 (2004) 82–88 (in Japanese).
- [16] H. Suzuki, S. Iizuka, Y. Hattori, K. Yuzawa, N. Matsumoto, Thin Solid Films 438–439 (2003) 288–293.
- [17] H. Suzuki, Mol. Cryst. Liq. Cryst. 370 (2001) 23–26.
- [18] H. Suzuki, Thin Solid Films 393 (2001) 352–357.
- [19] T.-W. Lee, O.O. Park, Appl. Phys. Lett. 77 (2000) 3334–3336.
- [20] H. Suzuki, S. Hoshino, Y. Nishida, Mol. Cryst. Liq. Cryst. 406 (2003) 221–231.
- [21] G.A. Crosby, R.E. Whan, R.M. Alire, J. Phys. Chem. 34 (1961) 743.
- [22] L.H. Slooff, A. van Blaaderen, A. Polman, G.A. Hebbink, S.I. Klink, F.C.J.M. Van Veggel, D.N. Reinhoudt, J.W. Hofstraat, J. Appl. Phys. 91 (2002) 3955–3980.
- [23] Optoelectronic Technology Roadmap for Optical Communication in 2002 (<http://www.oitda.or.jp/>).
- [24] M. Kuwata-Gonokami, K. Ema, K. Takeda, Mol. Cryst. Liq. Cryst. 216 (1992) 21.
- [25] T. Yamazaki, T. Tsutsui, Appl. Phys. Lett. 72 (1998) 1957–1959.
- [26] M. Notomi, H. Suzuki, T. Tamamura, Appl. Phys. Lett. 78 (2001) 1325–1327.
- [27] A. Yokoo, M. Notomi, H. Suzuki, M. Nakao, T. Tamamura, H. Masuda, IEEE J. Quantum Electron. 38 (2002) 938–942.
- [28] A. Yokoo, H. Suzuki, M. Notomi, Proceedings of the International Microprocesses and Nanotechnology Conference (MNC 2003), 30A-4-2, Tokyo, 2003.